Proceedings of the II Symposium on Positron Emission Tomography, Kraków, September 21–24, 2014

Perspectives for Highly-Sensitive PET-Based Medical Imaging Using $\beta^+\gamma$ Coincidences

P.G. Thirolf*, C. Lang and K. Parodi
Dep. of Medical Physics, Ludwig-Maximilians-Universität München,
Am Coulombwall 1, D-85748 Garching, Germany

By employing the triple coincidence between the γ trajectory intersections from β^+ decaying isotopes emitting a third, prompt, photon ("γ-PET" technique), sub-millimeter spatial resolution can be reached in 3 dimensions for the localization of a point source with a reduced requirement of reconstructed intersections per voxel compared to a conventional PET reconstruction analysis. Results of a Monte-Carlo simulation and image reconstruction study are presented in order to characterize the potential of this technique.

DOI: 10.12693/APhysPolA.127.1441
PACS: 87.57.uk, 87.57.N–, 87.57.C–

1. Introduction

So far a whole class of PET isotope candidates, where in addition to the two back-to-back emitted 511 keV β^+ annihilation photons a third, higher-energy γ ray will be emitted from an excited state in the daughter nucleus, has been excluded from medical application. The resulting extra dose delivered to the patient, as well as the expected increase of background from the Compton scattering or even pair creation, prevented the use of isotopes such as ^{44m}Sc, ^{86}Y, ^{94}Tc, ^{94m}Tc, ^{152}Tb, or ^{34m}Cl. However, provided the availability of customized gamma cameras, this alleged disadvantage could be turned into a promising benefit, offering a higher sensitivity for the reconstruction of the radioactivity distribution in PET examinations.

Table I lists the properties of presently used PET- or potential future γ-PET isotopes, including a comparison of the simulated positron diffusion range in water (last column) with measured values (column 6). Despite of their short halflives, ^{10}C (19.3 s) and ^{14}O (70.6 s) have been included here, since both can be produced during particle therapy irradiations, using carbon or proton beams [4, 5]. Thus they qualify as candidates for online ion-beam range monitoring during therapy treatment. Especially ^{44}Sc is of interest, which β^+-decays into the stable ^{44}Ca, emitting an 1157 keV photon. It has already been tested clinically [6]. With a short halflife of 3.9 h it has to be produced from a ^{44}Ti generator ($t_{1/2}$ = 60.4 a) [7], which presently cannot be performed in clinically relevant quantities. However, this may change with the expected future availability of highly brilliant γ beams [8].

2. Two approaches

Presently two approaches are pursued towards the realization of a medical imaging system based on β^+-γ coincidences. Both of them draw on the imaging properties of a Compton camera, where the registration of the Compton scatter (i.e. inelastic scattering of a photon with a (quasi-free) electron) and absorption kinematics of an incident photon in a suitable detection system is exploited to reconstruct the source position, within one event restricted to the surface of a cone (see Fig. 1a). Determining the intersection of this Compton cone with the line of response (LOR) as defined by the positron annihilation allows for a sensitive reconstruction of the decay position of the PET isotope (Fig. 1b). The intersection (Fig. 1b) of the Compton cone and the LOR strongly suppresses background and restricts the reconstructed events to those belonging to the same $\beta^+\gamma$ coincidence event, originating from a volume defined by the displacement between the positions of the β^+ decay and the positron annihilation, depending on the time resolution of the detector system.

Already in 2004, the XEMIS project started in France, aiming at realizing γ imaging by combining a PET scanner with a Compton camera based on a cryogenic time projection chamber (TPC) filled with liquid xenon (LXe), acting simultaneously as scatter, absorption and scintillation medium for the additional third photon [9]. A second, more conventional, experimental approach pursued in several European laboratories utilizes solid-state detectors to set up the Compton camera system [3, 10–13]. In the US, patents have been granted for the triple-γ technique [14, 15]. Typically, double-sided silicon strip detectors (DSSSD) or segmented CdZnTe detectors serve as the Compton scattering unit, while scintillation crystals (either from well-established materials like BGO or LSO, or from novel scintillators like $LaBr_3$), act as photon energy absorber. Such modules could be combined with a ring of PET detectors, alternatively a set of several Compton camera modules (as shown in Fig. 1a) could be arranged to detect either the β^+ annihilation photons or the additional γ photon in coincidence. A simulation study using the MEGAlib toolkit [16] based on GEANT4

*corresponding author; e-mail:
Peter.Thirolf@physik.uni-muenchen.de

TABLE I

Decay properties of presently used or potential future γ-PET isotopes. The positron diffusion range has been simulated with Geant4 (last column) and compared to experimentally measured values, where available.

	Decay mode	$E_{e^+}^{max}$ [MeV] [1]	I_β [%] [1]	E_γ [MeV] [1]	Mean range in water [mm] (exp. [2])	Mean range in water [mm] (sim. [3])
^{22}Na	$\beta^+ + \gamma$	0.54	100	1.27		1.5 ± 0.1
^{18}F	β^+	0.63	96.7		1.4	1.4 ± 0.1
^{94}Tc	$\beta^+ + \gamma$	0.81 1.83	10.5 70.8	0.87		1.4 ± 0.1
^{11}C	β^+	0.96	99.8		1.7	1.8 ± 0.1
^{13}N	β^+	1.20	100		2.0	1.9 ± 0.1
^{44}Sc	$\beta^+ + \gamma$	1.47	94.3	1.16		2.1 ± 0.1
^{15}O	β^+	1.73	99.9		2.7	2.6 ± 0.1
^{14}O	$\beta^+ + \gamma$	1.81	99.2	2.31		2.6 ± 0.1
^{68}Ga	$\beta^+ + \gamma$	1.90	88.0	1.08		2.7 ± 0.1
^{124}I	$\beta^+ + \gamma$	1.53 2.14	11.7 10.8	0.60		2.9 ± 0.1
^{10}C	$\beta^+ + \gamma$	2.93	98.5	0.72		2.6 ± 0.1
^{152}Tb	$\beta^+ + \gamma$	2.62 2.97	5.5 6.2	0.34		3.6 ± 0.1
^{86}Y	$\beta^+ + \gamma$	1.22 1.55 1.99 3.14	11.9 5.6 3.6 2.0	1.08		2.3 ± 0.1
^{76}Br	$\beta^+ + \gamma$	0.87 0.99 3.38 3.94	6.3 5.2 25.8 6.0	0.56		4.1 ± 0.1
^{82}Rb	$\beta^+ + \gamma$	4.39	100	0.78		4.9 ± 0.1

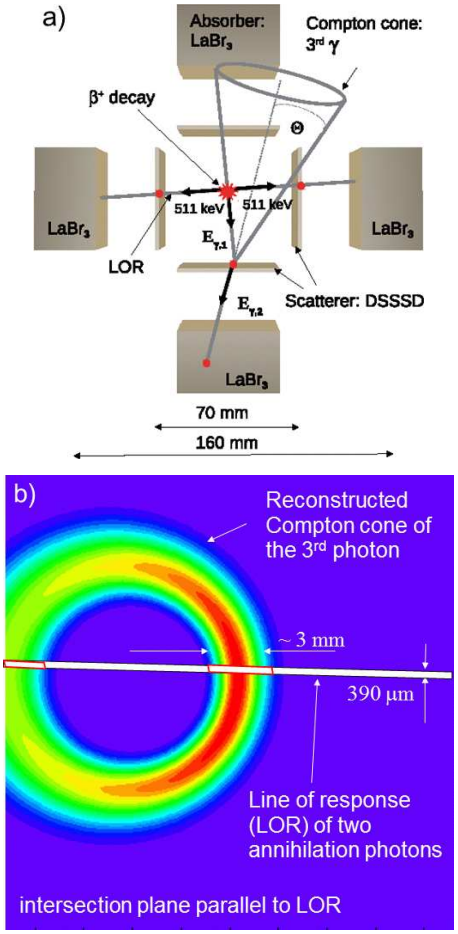

Fig. 1. Principle of the γ-PET technique (for details see text).

and a MLEM image reconstruction algorithm was conducted to evaluate the potential of the γ-PET technique when used with a Compton camera arrangement [3]. As shown in Fig. 1a, 4 Compton-camera based detector arms were used with a detector size of 5×5 cm^2 both for the scatter module (2 mm thick DSSSD, 128 strips per side, pitch 390 μm) as well as for the absorber detector (monolithic $LaBr_3$, $50 \times 50 \times 30$ mm^3, read out by a 16×16 segmented multianode PMT). A ^{22}Na point source was simulated in a distance of 5 cm from the scatter detectors (placed in the center of a water sphere with 6 cm diameter), reflecting a small-animal irradiation scenario. Alternatively, the reconstruction efficiency was also determined for an optimized geometry with a (stacked) thicker scatter detector (16 mm) and a larger absorber component, covering the full opening angle of the cone seen from the photon source placed at the top of a pyramid. This would require an absorber with an area of 114×114 mm^2.

Table II lists the simulated reconstruction efficiencies for these two geometries and different γ-PET isotopes. In order to study the achievable position resolution with γ-PET, an arrangement of 12 ^{22}Na sources positioned

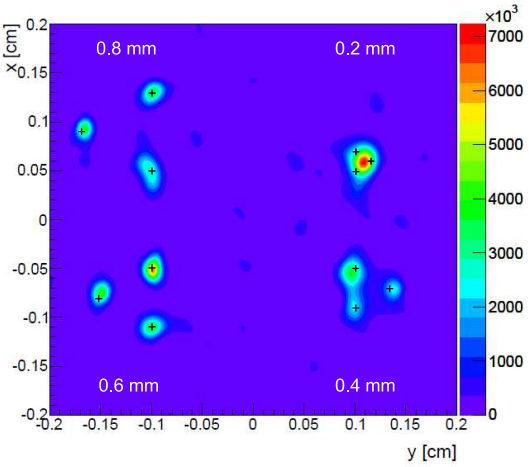

Fig. 2. Image of the reconstructed γ-source geometry of 12 ^{22}Na point sources, arranged in equilateral triangles with spacings of 0.2, 0.4, 0.6, and 0.8 mm. The γ-PET technique was applied with 100 iterations using a maximum-likelihood algorithm. The black crosses indicate the original source positions.

in 4 equilateral triangles, with spacings of 0.2, 0.4, 0.6, and 0.8 mm, respectively, was simulated. As can be seen in Fig. 2, even for the case of a source spacing of 0.4 mm the source images can still be resolved, proving sub-millimetric resolution for this reconstruction scenario.

TABLE II

Simulated reconstruction efficiencies for various $\beta^+ - \gamma$ emitters. In case of ^{124}I and ^{76}Br, which emit several prompt γ rays with considerable branching ratio, the individual efficiencies have been summed up (^{124}I: 0.60, 0.72, 1.5 and 1.7 MeV. ^{76}Br: 0.56, 0.66, 1.13, 1.22 and 1.85 MeV). The upper line corresponds to the detector system shown in Fig. 1a), while the lower line represents the reconstruction efficiency for an optimized system with thicker scatter and larger absorber detectors (see text).

Isotope	^{22}Na	^{44}Sc	^{14}O	^{68}Ga	^{124}I	^{10}C	^{76}Br	^{82}Rb
$\epsilon_{\mathrm{rec},1}$ [10^{-8}]	7.0	6.0	1.6	0.093	20	6.8	47	2.6
$\epsilon_{\mathrm{rec},2}$ [10^{-5}]	9.7	8.0	5.1	0.13	22	2.8	89	3.3

3. γ-PET method

The particular advantage of the γ-PET method becomes evident when assessing its sensitivity. In order to compare the performance of the γ-PET technique with conventional PET, we determined the imaging sensitivity of the method based on a comparable width of the LOR of *ca.* 2 mm. In a standard PET Iterative Reconstruction analysis (without exploiting time-of-flight information), about 6000 true coincidences acquired with a Siemens Biograph mCT PET scanner are necessary to localize a ^{22}Na point source in the center of the scanner field-of-view using the smallest voxel volume of $2\times2\times3$ mm^3 [3]. Already 40 reconstructed intersections per voxel (derived without iterative reconstruction procedure) lead to a reliable localization of the ^{22}Na point source. This sensitivity can be evaluated and compared to standard PET imaging by quantifying the examination time required to localize a point source as described above. The minimum number of β^+-emitter decays per voxel N_{decay}, required for localizing a point source, relates to the imaging sensitivity, expressed by the minimum number of reconstructed intersections N_{inter} and the corresponding reconstruction efficiency ϵ_{rec} as well as to the activity concentration $C(i)$ of each voxel i, the examination time Δt and the voxel volume V_{vox} according to

$$N_{\mathrm{decay}}(i) = N_{\mathrm{inter}}(i)/\epsilon_{\mathrm{rec}} = C(i)\Delta t V_{\mathrm{vox}}(i). \quad (1)$$

For a given activity concentration and tumor size, the required examination time for localizing a point source only depends on the imaging sensitivity N_{inter} and the reconstruction efficiency ϵ_{rec}. While the γ-PET method described here indicates a clear advantage in terms of sensitivity expressed by N_{inter} compared to standard PET, it falls behind when comparing the corresponding efficiencies ϵ_{rec}, where values of about 0.1 are reported for small-animal PET scanners [17] and similar values are found for whole-body scanners [18].

Table III lists in the last column the examination times τ^{exam} required for the localization of point sources of selected γ-PET radioisotopes, where information of tracer and associated equivalent dose coefficients (h_T) were available. τ^{exam} reflects the imaging sensitivity of the γ-PET method based on the minimum requirement of 40 reconstructed intersections and the isotope-specific reconstruction efficiencies $\epsilon_{\mathrm{rec},2}$ (see Table II). A typical value for the activity concentration accumulated in a tumor of 25 kBq/ml was assumed, corresponding to a PET examination of a patient with a body weight of 80 kg with an injected dose of 400 MBq and an average SUV (standard uptake value) of 5 [3]. Column 7 shows the corresponding effective dose values (calculated with h_T values derived for adult males).

TABLE III

γ-PET examination time τ^{exam} for the localization of a point source of selected $\beta^+\gamma$-decaying radioisotopes, assuming an injected activity of 400 MBq and a tumor activity concentration of 25 kBq/ml. τ^{exam} reflects the imaging sensitivity of the γ-PET method based on the minimum requirement of 40 reconstructed intersections and the isotope-specific reconstruction fficiencies $\epsilon_{\mathrm{rec},2}$. Column 7 shows the corresponding effective dose $\mathrm{E}^{\mathrm{exam}}$, based on the associated equivalent dose coefficients h_T (for adult males). The first columns list decay properties and suitable tracers of the respective isotopes.

	$t_{1/2}$ [min]	γ/β^+ [%]	Tracer	h_T $\left[\frac{\mu\mathrm{Sv}}{\mathrm{MBq}}\right]$	Ref.	E^{exam} [mSv]	τ^{exam} [s]
^{14}O	1.2	99	Water	0.88	[19]	0.33	2420
^{124}I	6013	90	MIBG	250	[20]	92	558
^{76}Br	16.2	100	MAb-38S1	410	[21]	150	138
^{82}Rb	1.3	13	Chloride	1.28	[22]	0.46	3740
^{44}Sc	236		DOTATOC	n.a.	[7]		1100

4. Conclusion

The concept of 3 γ coincidence imaging ("γ-PET") may open up the perspective to exploit a whole class of new PET isotopes, offering a highly sensitive and highly resolving localization of the photon source position. Development efforts should be directed towards optimizing the reconstruction efficiency achievable with γ-PET in order to mitigate the present detection efficiency limitation compared to standard PET imaging. Moreover, the Compton camera arrangement described here could also turn out to be beneficial in a therapeutic hadron beam irradiation, where $\beta^+(\gamma)$ emitters (^{10}C, ^{14}O) are generated via, e.g., a carbon beam and could be exploited to reconstruct their spatial distribution within the patient, either from a (quasi-realtime) PET analysis (i.e. direct reconstruction using TOF-PET) or using the hybrid γ-PET technique to achieve an improved spatial resolution together with an enhanced sensitivity, i.e. reduced requirements to the irradiation-induced activity strength.

Acknowledgments

This work was supported by the DFG Cluster of Excellence MAP (Munich-Centre for Advanced Photonics). Fruitful discussions with D. Habs, C. Kurz, and G. Böning are particularly acknowledged.

References

[1] M.R. Bhat, *Nuclear Data for Science and Technology*, Ed. S.M. Quain, Springer-Verlag, Berlin 1992, p. 817.

[2] J.L. Humm, A. Rosenfeld, A. Del Guerra, *Eur. J. Nucl. Med. Mol. Imaging* **30**, 1574 (2003).

[3] C. Lang, D. Habs, K. Parodi, P.G. Thirolf, *J. Inst.* **9**, P01008 (2014).

[4] F. Sommerer, F. Cerutti, K. Parodi, A. Ferrari, W. Enghardt, H. Aiginger, *Phys. Med. Biol.* **54**, 3979 (2009).

[5] K. Parodi, A. Ferrari, F. Sommerer, H. Paganetti, *Phys. Med. Biol.* **52**, 3369 (2007).

[6] F. Rösch, R.P. Baum, *Dalton Trans.* **40**, 6104 (2011).

[7] M. Pruszyński, N.S. Loktionova, D.V. Filosofov, F. Rösch, *Appl. Radiat. Isot.* **68**, 1636 (2010).

[8] D. Habs, U. Köster, *Appl. Phys. B* **103**, 501 (2011).

[9] C. Grignon, J. Barbet, M. Bardiés, T. Carlier, J.F. Chatal, O. Couturier, J.P. Cussonneau, A. Faivre, L. Ferrer, S. Girault, T. Haruyama, P. Le Ray, L. Luquin, S. Lupone, V. Métivier, E. Morteau, N. Servagent, D. Thers, *Nucl. Instrum. Methods Phys. Res. A* **571**, 142 (2007).

[10] J. Donnard, W.-T. Chen, J.P. Cussonneau, S. Duval, J. Lamblin, O. Lemaire, A.F. Mohamad Hadi, P. Le Ray, E. Morteau, T. Oger, L. Scotto Lavina, J.-S. Stutzmann, D. Thers, *Nucl. Med. Rev. Suppl. C* **15**, C64 (2012).

[11] T. Kormoll, F. Fiedler, S. Schöne, J. Wüstemann, K. Zuber, W. Enghardt, *Nucl. Instrum. Methods Phys. Res. A* **626–627**, 114 (2011); *Radiother. Oncol.* **102**, s41 (2012).

[12] F. Roellinghoff, M.-H. Richard, M. Chevalier, J. Constanzo, D. Dauvergne, N. Freud, P. Henriquet, F. Le Foulher, J.M. Letang, G. Montarou, C. Ray, E. Testa, M. Testa, A.H. Walenta, *Nucl. Instrum. Methods Phys. Res. A* **648**, s20 (2011).

[13] C. Lang, D. Habs, A. Zoglauer, P.G. Thirolf, *Radiother. Oncol.* **102(1)**, s30 (2012).

[14] E. Gonzalez, P.D. Olcott, M. Bieniosek, C.S. Levin, *IEEE NSS-MIC Conf. Rec.*, 3597 (2011).

[15] C.S. Levin, US patent application 20090072156 (2009).

[16] A. Zoglauer, R. Andritschke, F. Schopper, *New Astron. Rev.* **50**, 629 (2006).

[17] E.P. Visser, J.A. Disselhorst, M. Brom, P. Laverman, M. Gotthardt, W.J.G. Oyen, O.C. Boerman, *J. Nucl. Med.* **50**, 139 (2009).

[18] L. Eriksson, D. Townsend, M. Conti, M. Eriksson, H. Rothfuss, M. Schmand, M.E. Casey, B. Bendriem, *Nucl. Instrum. Methods Phys. Res. A* **580**, 836 (2007).

[19] M. Sajjad, M.R. Zaini, J.-S. Liow, D.A. Rottenberg, S.C. Strother, *Appl. Radiat. Isot.* **57**, 607 (2002).

[20] C.-L. Lee, H. Wahnishe, G.A. Sayre, H.-M. Cho, H.-J. Kim, M. Hernandez-Pampaloni, R.A. Hawkins, S.F. Dannoon, H.F. Vanbrocklin, M. Itsara, W.A. Weiss, X. Yang, D.A. Haas-Kogan, K.K. Matthay, Y. Seo, *Med. Phys.* **37**, 4861 (2010).

[21] A. Lövqvist, H. Lundqvist, M. Lubberink, V. Tolmachev, J. Carlsson, A. Sundin, *Med. Phys.* **26**, 249 (1999).

[22] S. Senthamizhchelvan, P.E. Bravo, M.A. Lodge, J. Merrill, F.M. Bengel, G. Sgouros, *J. Nucl. Med.* **52**, 485 (2011).